Structures and Interaction with DNA of Ternary Palladium(II) Complexes: [Pd(Gly)(X)] (Gly=Glycine; X=2,2′-Bipyridine, 1,10-Phenanthroline and 2,2′-Bi-pyridylamine)

Masahiro YODOSHI and Nobuo OKABE*

Faculty of Pharmaceutical Sciences, Kinki University; 3–4–1 Kowakae, Higashi-osaka, Osaka 577–8502, Japan.
Received January 19, 2008; accepted April 2, 2008; published online April 15, 2008

The structures of the ternary palladium(II) complexes of the formulations $[Pd(Gly)(bpy)]^+Cl^-\cdot 4H_2O$ (Gly=glycine; bpy=2,2′-bipyridine) (1), $[Pd(Gly)(phen)]^+Cl^-\cdot 4H_2O$ (2) (phen=1,10-phenanthroline) and $\{[Pd(Gly)(bpa)]^+Cl^-\}_2\cdot 6H_2O$ (3) (bpa=2,2′-bipyridylamine) were determined. All complexes are positively charged and neutralized by the chloride anion located nearby the complexes. The central Pd(II) atoms of the complexes 1, 2 and 3 have a similar distorted square planar coordination geometry, in which each Pd(II) atom is coordinated to two N atoms of the bidentate heterocyclic ligand, and N and O atoms of the bidentate glycine ligand. The interaction of the complexes with calf thymus (CT) DNA was also studied using the fluorescence method. All complexes showed the inhibition of ethidium bromide binding to CT DNA, and the DNA-binding strengths were reflected as the relative order 2>1>3. The remarkable reduction of UV absorption intensity of 2 caused in the presence of DNA suggests the presence of π–π stacking interaction between the heterocyclic ring of the phen ligand and nucleobases. The intercalative DNA-binding of 2 is suggested by UV and CD measurements. DNA cleavage studies indicated that the cleavage of the plasmid supercoiled pBR322 DNA in the presence of H_2O_2 and ascorbic acid could be enhanced by the complexes.

Key words crystal structure; palladium(II) complex; DNA cleavage; 2,2′-bipyridine; 1,10-phenanthroline; 2,2′-bipyridylamine

Following the discovery of *cis*-diamminedichloroplatinum(II) (cisplatin) as the successful antitumor drug,[1] the research of the design and synthesis of novel platinum(II) complexes, having more favorable antitumor activities as compared with cisplatin, has been continued.[2—5] Palladium(II) complexes have been also investigated for developing the new antitumor agents,[6—12] because palladium(II) has a similar coordination mode and chemical properties to platinum(II).[12] As the result, several novel palladium(II) complexes having antitumor citotoxic activities against MCF-7, TK-10 and UACC-62 human tumor cell lines,[13] and P388 lymphocytic leukemia cells have been found.[14—17] In these complexes, the ternary palladium(II) complexes with a heterocyclic ligand and L-glycine one, [Pd(Gly)(X)] (where X is a heterocyclic ligand; 2,2′-bipyridylamine(bpa),[15] 1,10-phenanthroline (phen)[16] and 2,2′-bipyridine(bpy)[17]) have the antitumor activity against P388 lymphocytic leukemia cells. At the present time, the structures of these complexes are not yet clear, although they are important for clarifying the mechanism of their antitumor activity. By these circumstances, in this study, our aim was to determine the structures of three ternary Pd(II) complexes, $[Pd(Gly)(bpy)]^+Cl^-\cdot 4H_2O$ (**1**), $[Pd(Gly)(phen)]^+Cl^-\cdot 4H_2O$ (**2**) and $\{[Pd(Gly)(bpa)]^+Cl^-\}_2\cdot 6H_2O$ (**3**), and evaluate the interaction with DNA, which is one of targets in the chemotherapy of tumor.[18]

Experimental

Materials Analytical grade of 2,2′-bipyridine (bpy), 1,10-phenanthroline (phen), and 2,2′-bipyridylamine (bpa), L-glycine (Gly), palladium(II) chloride disodium chloride trihydrate, other reagents and Agarose-Precast Gel (1%) were obtained from Wako Pure Chemicals, Industries Ltd. (Osaka, Japan). Calf thymus DNA (CT DNA) and super coiled plasmid pBR322 DNA (SC DNA: Lot No. K4301A) were obtained from SIGMA (St. Louise, MO, U.S.A.) and TAKARA BIO INC. (Otsu, Japan), respectively. Gene Ruler 100 bp DNA Lader Plus and Loading Dye solution (Fermentas Co., Ltd.) were obtained from COSMO BIO Co., Ltd. (Tokyo, Japan).

Methods The X-ray measurements were performed on a Rigaku R-AXIS RAPID diffractometer with a graphite monochromatized Mo$K\alpha$ radiation (λ=0.71069 Å) using the ω scan mode at 123.1 K.

Fluorescence measurements were performed with a Hitachi 850 spectrofluorometer. UV measurements were made on a Shimazu Pharma Spec UV-1700 Spectrophotometer and CD measurements on a JASCO J-710 CD spectrophotometer. The agarose gel electrophoresis was performed using a COSMO BIO Mupid-2. Elemental analysis was done by using a YANACO CHN Coder MT-3.

Preparation of the Complexes The complex **1**, **2** and **3** were prepared according to the analogous method described previously.[15,19]

0.76 mmol of bpy, phen or bpa were mixed with 0.76 mmol of $PdCl_2\cdot 2NaCl\cdot 3H_2O$ in 5 ml of 80% (v/v) methanol–water solution for about 5 min at room temperature. The precipitates appeared after adding palladium salt. Each precipitate was dried under a vacuum and assumed as $[Pd(bpy)Cl_2]$, $[Pd(phen)Cl_2]$ and $[Pd(bpa)Cl_2]$. Then, 0.015 mmol of the precipitate was reacted with equal moles of Gly and $NaHCO_3$ in 5 ml of water solution for about 1 h at 333—343 K, until the volume of the reaction mixture was concentrated to *ca.* 1 ml. The concentrated solution was allowed to stand at room temperature for slow evaporation. Two weeks later, the light yellow needle crystals of the complex **1** and **3** suitable for X-ray diffraction studies were obtained from the mother liquid, and three months later the brown needle crystal of the complex **2** was obtained.

The results of the elemental analyses of the complexes were as follows:

Complex **1**: *Anal.* Calcd for $[Pd(Gly)(bpy)]^+Cl^-\cdot 4H_2O$: C, 32.452; H, 4.539; N, 9.463. Found: C, 32.486; H, 4.378; N, 9.612.

Complex **2**: *Anal.* Calcd for $[Pd(Gly)(phen)]^+Cl^-\cdot 4H_2O$: C, 35.918; H, 4.306; N, 8.978. Found: C, 36.089; H, 4.158; N, 9.025.

Complex **3**: *Anal.* Calcd for $\{[Pd(Gly)(bpa)]^+Cl^-\}_2\cdot 6H_2O$: C, 32.377; H, 5.208; N, 12.589. Found: C, 32.445; H, 5.299; N, 12.712.

X-Ray Crystallography The data was corrected for Lorentz and polarization effects. The structure was solved by direct methods[20] using the Crystal Structure[21] software package. The refinement was performed using SHELXL-97.[22] All H atoms including water molecules were located from difference Fourier maps and placed at idealized positions and treated as riding, with C–H distance of 0.93 and U_{iso}(H) values equal to 1.2 U_{eq}(C) and U_{iso}(water H) values equal to 1.5 U_{eq}(C) (U_{eq} is the equivalent isotropic displacement parameter for the pivot atom). The function of $\sum w(F_o^2-F_c^2)^2$ was minimized by using the weight scheme of $w=1/[\sigma^2(F_o^2)+(aP)^2+bP]$, where $P=(F_o^2+2F_c^2)/3$. The crystallographic data, including final R [$=\sum(|F_o|-|F_c|)/\sum|F_o|$], Rw [$=(\sum w(|F_o|-|F_c|)^2/\sum w|F_o|^2)^{1/2}$], and S (goodness of fit) [$=(\sum w(|F_o|-|F_c|)^2/(M-N)^{1/2}$), where M=no. of reflections and N=no. of variables used for the refinement] values are given in Table 1.

* To whom correspondence should be addressed. e-mail: okabe@phar.kindai.ac.jp

Table 1. Crystal Data and Structure Refinement for the Complexes **1**—**3**

	1	**2**	**3**
Formula	$C_{12}H_{12}N_3O_2PdCl \cdot 4H_2O$	$C_{14}H_{12}N_3O_2PdCl \cdot 4H_2O$	$\{C_{12}H_{12}N_4O_2PdCl\}_2 \cdot 6H_2O$
Formula weight	444.18	468.20	882.36
Crystal system	Orthorhombic	Orthorhombic	Triclinic
Space group	$Pca2_1$	$Pbca$	$P\bar{1}$
a (Å)	24.23(2)	22.03(2)	6.931(7)
b (Å)	9.90(1)	6.724(4)	11.35(2)
c (Å)	7.002(7)	23.56(1)	20.89(2)
α (°)	90.00	90.00	81.22(4)
β (°)	90.00	90.00	81.46(3)
γ (°)	90.00	90.00	86.99(4)
V (Å^3)	1680(3)	3489(4)	1605(4)
Z	4	8	2
D calc (g/cm^{-3})	1.704	1.782	1.826
T (K)	123.1	123.1	123.1
F(000)	896	1888	888
Crystal size (mm)	0.40×0.10×0.10	0.35×0.04×0.04	0.55×0.06×0.06
Absorption coefficient (mm^{-1})	1.296	1.253	1.353
Unique	3729	4020	7334
R ($F^2>2\sigma(F^2)$)	0.017	0.045	0.041
wR (F^2)	0.045	0.120	0.130
Goodness of fit	1.023	0.971	1.085
No. of variables	209	227	416

Anisotropic displacement coefficients were refined for all non-hydrogen atoms. Selected bond distances and angles are listed in Table 2.

The final atomic coordinates, anisotropic displacement coefficients, bond lengths, bond angles, torsion angles of non-H atoms, and the atomic coordinates of H atoms have been deposited in the Cambridge Crystallographic Data Centre, Cambridge University Chemical Laboratory, Cambridge CB21EW, U.K. (CCDC No. 639517 for $[Pd(Gly)bpy)]^+Cl^-\cdot 4H_2O$ (**1**), CCDC 639518 for $[Pd(Gly)(phen)]^+Cl^-\cdot 4H_2O$ (**2**), CCDC 639519 for $\{[Pd(Gly)(bpa)]^+Cl^-\}_2\cdot 6H_2O$ (**3**).

DNA-Binding and Cleavage Experiments The binding experiment of the complexes to CT DNA was studied using the fluorescence method. Competitive binding studies were performed by measuring the emission of ethidium bromide (EB) bound to DNA, which shows enhanced emission intensity due to its intercalative binding to DNA.[23,24] The competitive binding of the complexes to DNA reduces the emission intensity of EB with either a displacement of the bound EB from the bound to the free state or the bound complex quenching the emission.[25,26]

In a typical binding experiment, a 2 μl solution of 1.45 mM EB was added to a volume of 300 μl of 100 μM CT DNA solution. An aliquot of 3 mM solution of the complexes in distilled water was added to the EB-DNA solution. After the mixtures were incubated overnight for equilibration at 298 K, fluorescence measurements were taken at λ_{ex} of 545 nm and λ_{em} of 600 nm at 298 K.

The fluorescence intensities at 600 nm were plotted against the complex concentration to yield a slope that showed the relative extent of binding of the complexes to DNA. A control experiment was also done with the EB in the absence of DNA for correcting the fluorescence intensity.

Absorption spectra of the complexes were measured in similar conditions with the fluorescence measurements. At this time, the final concentration of the complex was 10 μM, and those of CT-DNA were 20—150 μM, at which the molar ratios of [DNA]/[Complex]=R were changed as 2, 5, 10 and 15. The mixtures of the complex and DNA were equilibrated overnight at 298 K before measurements. The absorption spectra of the mixture were measured at the wavelength region of 220—340 nm at 298 K, and the difference spectra were obtained by subtracting the absorption of DNA from that of the mixture.

CD measurements were made at similar conditions with the absorption and fluorescence measurements in 10 mM Tris–HCl buffer, pH 7.4, containing 50 mM NaCl. The final concentrations of CT DNA and the complex are 150 μM and 50 μM, at which the molar ratio of [DNA]/[Complex]=R was 3. The mixtures of the complex and DNA were equilibrated overnight at 298 K before measurements. The CD spectra of the mixture were measured at the wavelength region of 240—320 nm at 298 K.

Table 2. (a) Selected Bond Distances (Å) and Angles (°) for the Complexes **1**—**3** with e.s.d.s in Parenthesis

Complex **1**

Bond distances		Bond angles	
Pd1–O1	1.987(2)	O1–Pd1–N1	175.87(7)
Pd1–N1	2.005(2)	O1–Pd1–N2	93.04(8)
Pd1–N2	2.008(2)	O1–Pd1–N3	83.02(7)
Pd1–N3	2.036(2)	N1–Pd1–N2	81.07(7)
		N1–Pd1–N3	101.04(7)
		N2–Pd1–N3	177.89(7)

Complex **2**

Bond distances		Bond angles	
Pd1–O1	1.993(3)	O1–Pd1–N1	176.6(2)
Pd1–N1	2.020(4)	O1–Pd1–N2	94.7(2)
Pd1–N2	2.007(4)	O1–Pd1–N3	82.8(2)
Pd1–N3	2.028(4)	N1–Pd1–N2	82.1(2)
		N1–Pd1–N3	100.5(2)
		N2–Pd1–N3	177.2(2)

Complex **3**

Bond distances		Bond angles	
Pd1–O1	2.007(3)	O1–Pd1–N1	177.5(1)
Pd1–N1	2.003(4)	O1–Pd1–N2	91.6(1)
Pd1–N2	2.000(4)	O1–Pd1–N4	82.5(1)
Pd1–N4	2.044(4)	N1–Pd1–N2	90.6(7)
Pd2–O3	2.008(4)	N1–Pd1–N4	95.2(2)
Pd2–N5	2.013(4)	N2–Pd1–N4	173.4(2)
Pd2–N6	2.012(4)	O3–Pd2–N5	91.5(1)
Pd2–N8	2.051(4)	O3–Pd2–N6	175.9(2)
		O3–Pd2–N8	81.6(2)
		N5–Pd2–N6	90.7(2)

The cleavage experiments were performed by the gel electrophoresis using SC DNA in 10 mM Tris–HCl buffer, pH 7.4, containing 50 mM NaCl.[13,15] The reaction mixtures were prepared as follows: both 4 μl of 7 mM H_2O_2 and 4 μl of 7 mM ascorbic acid were added to a mixture of 20 μl of SC DNA (0.05 μg/μl) and 6 μl of 300 μM complexes, followed by dilution with Tris–HCl buffer to a total volume of 40 μl. The final concentration of the complexes was 45 μM, and that of H_2O_2 and ascorbic acid was 525 μM. The reactions were performed after incubating the reaction mixture at 298 K for 1 h in the presence and/or absence of the complexes. For the experiments on the concentration dependence of the complexes, 3 μl of H_2O_2, 3 μl of H_2O_2 and 2—10 μl of the complexes were used in the above reaction mixture of total 40 μl. The final concentrations of the complexes were changed from 15 to 75 μM, and that of H_2O_2 and ascorbic acid was 525 μM.

A loading buffer (3 μl) containing 0.03% bromophenol blue, 0.03% xylene cyanol, and 60% glycerol was added to 20 μl of the reaction mixture and electrophoresis was performed at 50 V for 70 min in Tris–acetate–EDTA (TAE) buffer, pH 8.1, using 1% agarose gel. After electrophresis, the agarose gel was dyed in EB solution (0.5 μg/ml).

The cleavage of SC DNA was monitored by photographing the fluorescence of intercalated EB using Amersham Pharmacia Biotech Image Master VDS-CL illuminator.

The concentration of CT DNA was determined by measuring the absorption intensity at 260 nm with the molar extinction coefficient value of 6600 M^{-1} cm^{-1} in 10 mM Tris–HCl buffer, pH 7.4, containing 50 mM NaCl.[27] The concentration of SC DNA was calculated from the contents of the sample vials (0.5 μg/μl).

Results and Discussion

Crystal Structures The structure of the complex **1** is shown in Fig. 1a. The Pd(II) atom has a distorted square-planar four-coordination geometry and is bonded to two heterocyclic N atoms, and an N atom and an O atom from Gly in a equatorial plane. The complex itself is positively charged, and neutralized by free Cl^- anion located nearby. In the square-planar coordination, the rms deviation of Pd1 from

the mean plane through O1, N1, N2 and N3 atoms is 0.006(1) Å. The five membered chelate rings, Pd1–N1–C5–C6–N2 and Pd1–O1–C11–C12–N3, are formed with bpy and Gly ligand, respectively. These rings are almost planar with the dihedral angle between the planes Pd1–N1–N2 and Pd1–N3–O1 of 0.76(9)°. Two pyridine rings of bpy ligand are also planar with the dihedral angle of 0.4(3)°. The Gly takes a eclipsed conformation with a little large torsion angle, N3–C11–C12–O1, ±17.1(3)°. This may be caused by the steric hindrance between the H atom of C1 and the H atom of the amino group.

The packing pattern of **1** with the hydrogen-bond networks is shown in Fig. 1b.

The complex molecules are connected by the hydrogen bond network through hydrated water molecules and Cl^- atom. The Cl^- atom acts as the acceptor of the four hydrogen bonds. The π–π interaction is present between bpy ligands related by the crystallographic symmetry. The distance between Cg1(N1/C1/C2/C3/C4/C5) [symmetry code: $(+x, +y, +z)$] and Cg2(N2/C6/C7/C8/C9/C10) [symmetry code: $(3/2-x, +y, 1/2+z)$] is 3.759(7) Å, where Cg indicates the center of the gravity (Cg) of the ring.

The stacking layer arrays along *c* axis. The overall complex molecules are stabilized by the H-bond networks together with the π–π interactions.

The structure of the complex **2** is shown in Fig. 2a. The coordination geometry and atoms around the central Pd(II) atom is the same with **1**. The rms deviation of Pd1 from the mean square plane (N1/N2/O1/N3) is 0.004(2) Å as similar to **1**. The dihedral angle between (N1/Pd1/N2) and (N3/Pd1/O1) planes is 1.416(6)°. The Gly ligand takes an eclipsed conformation with torsion angle, N3–C13–C14–O1, is ±11.8(7)°. The phen ring is planar.

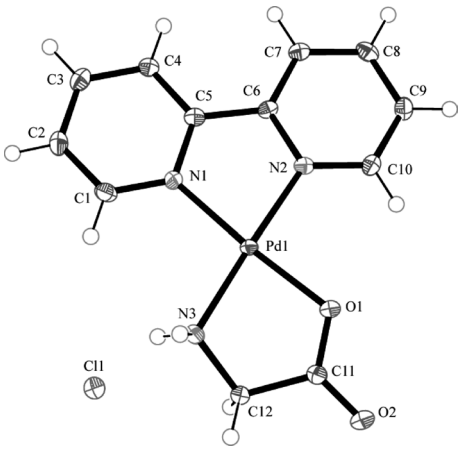

Fig. 1a. ORTEPIII Drawing of the Complex **1**, Showing 50% Probability Displacement Ellipsoids

The water molecules involved in the unit are omitted for the clarification of the basic Pd(II) coordination geometry.

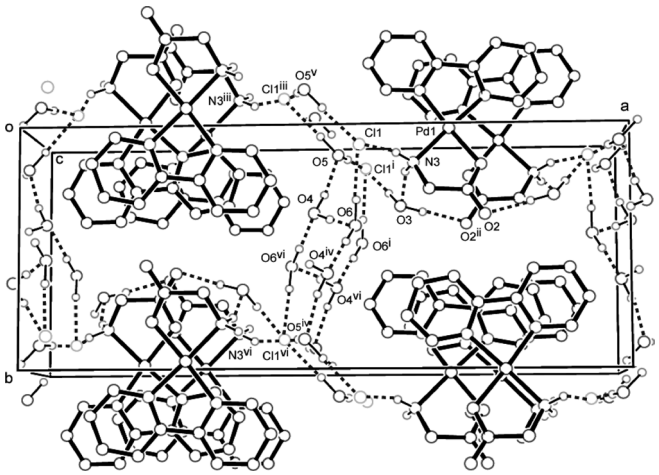

Fig. 1b. A View of Packing Pattern in the Complex **1** Including H-Bond Networks Indicated by Dashed Lines

i: $+x, +y, 1+z$, ii: $3/2-x, +y, 1/2+z$, iii: $1-x, -y, 1/2+z$, iv: $1-x, 1-y, -3/2+z$, v: $1-x, -y, -1/2+z$, vi: $1-x, 1-y, 1/2+z$.

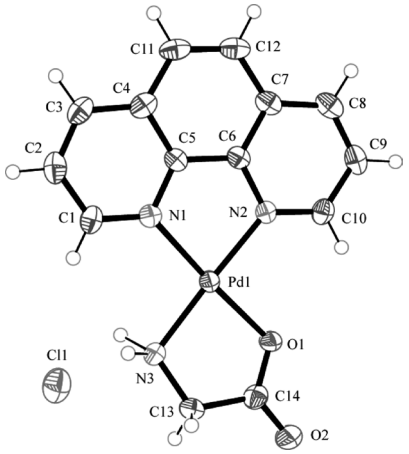

Fig. 2a. ORTEPIII Drawing of the Complex **2**, Showing 50% Probability Displacement Ellipsoids

The water molecules involved in the unit are omitted for the clarification of the basic Pd(II) coordination geometry.

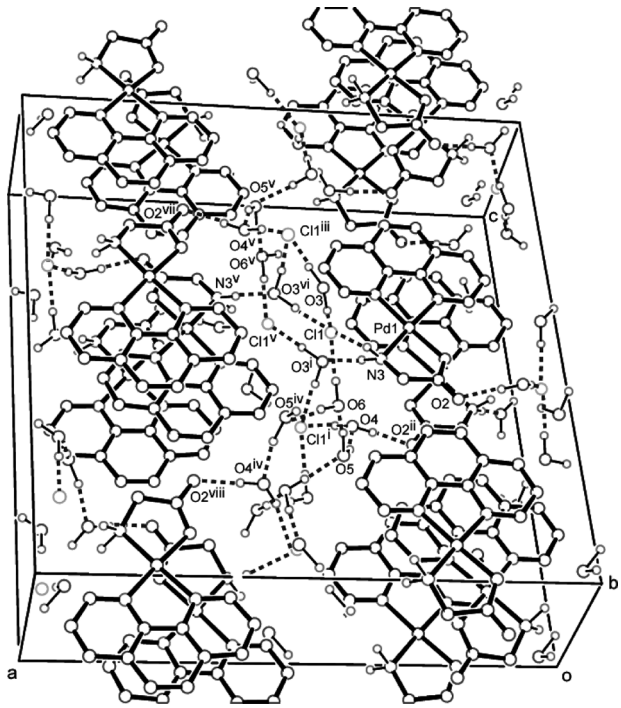

Fig. 2b. A View of Packing Pattern in the Complex **2** Including H-Bond Networks Indicated by Dashed Lines

i: $+x, -1+y, +z$, ii: $1/2-x, -1/2+y, +z$, iii: $1-x, 1-y, 1-z$, iv: $-x, 1/2+y, 1/2-z$, v: $1-x, -y, 1-z$, vi: $1-x, 1-y, 1-z$, vii: $1/3+x, 1/2-y, 1-z$, viii: $1/2+x, +y, 1/2-z$.

The packing pattern of **2** with the hydrogen-bond networks is shown in Fig. 2b.

The complex molecules are connected to each other by the available H-bonds. The π–π interaction is also present between phen rings with the distances between Cg1(N2/C6/C7/C8/C9/C10) and Cg2(C4/C5/C6/C7/C11/C12) [symmetry code: $(1/2-x, 1/2+y, +z)$] of 3.643(4) Å. The overall complex molecules are stabilized by the H-bond network together with the π–π interaction.

The structure of the complex **3** is shown in Fig. 3a. Two independent complex molecules are present in an asymmetric unit. Their coordination geometries resemble each other, and both Pd1 and Pd2 have a distorted square-planar four coordination geometry like the complexes **1** and **2**. Ligand atoms are also the same as **1** and **2**. Two Cl^- anions locate nearby the complex. Each Pd atom deviates from the mean square planes (N1/N2/O1/N4) and (N5/N6/O3/N8) by 0.036(2) Å and 0.028(2) Å, respectively. The six membered chelate rings, Pd1–N1–C5–N3–C6–N2 and Pd2–N5–C17–N7–C18–N6 are formed with bpa ligands, and five membered rings with Gly ligands. The two pyridine rings of bpa ligand of each complex are slightly twisted with the dihedral angle 20.5(2)° and 20.3(2)° for Pd1 and Pd2 complex, respectively. This may be caused by the short contact between the H atom of C1 and the H atom of the amino group as in the case of **1** and **2**. The Gly ligand takes an eclipsed conformation with the torsion angle N4–C11–C12–O1, ±8.7(7)° and N8–C23–C24–O3, ±11.9(7)°.

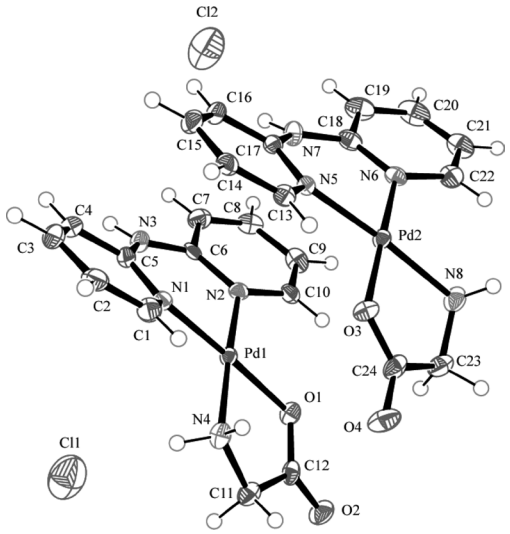

Fig. 3a. ORTEPIII Drawing of the Complex **3**, Showing 50% Probability Displacement Ellipsoids

The water molecules involved in the unit are omitted for the clarification of the basic Pd(II) coordination geometry.

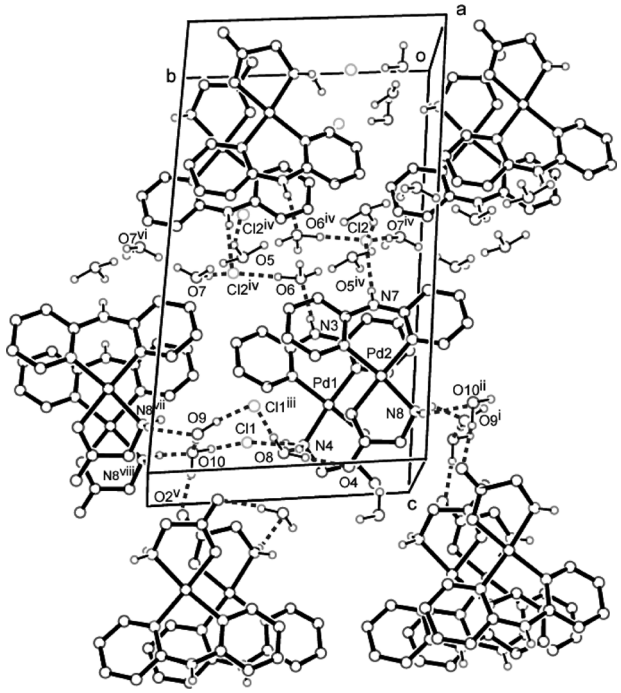

Fig. 3b. A View of Packing Pattern in the Complex **3** Including H-Bond Networks Indicated by Dashed Lines

i: $+x, -1+y, +z$, ii: $1+x, -1+y, +z$, iii: $1+x, +y, +z$, iv: $1-x, 1-y, 1-z$, v: $-x, 1-y, 2-z$, vi: $1-x, 2-y, 1-z$, vii: $+x, 1+y, +z$, viii: $-1+x, 1+y, +z$.

The packing pattern of the complex **3** with the hydrogen-bond network is shown in Fig. 3b, where the H atoms attached to the hydrated water O5, O6 and O7 atoms disordered. Available H-bond networks are formed through water molecules, Cl^- atoms and the NH group of bpa. The face to face π–π interactions are present between bpa ligands with distances of 3.630(6) Å for the stacking between Cg1(N1/C1/C2/C3/C4/C5) and Cg2(N5/C13/C14/C15/C16/C17) [symmetry code: $(+x, +y, +z)$], and 3.838(6) Å for Cg3(N2/C6/C7/C8/C9/C10) and Cg4(N6/C18/C19/C20/C21/C22). The overall complex molecules are stabilized by the H-bond network together with the π–π interaction.

In all of the complex molecules, the Pd(II) atom has a distorted square-planar four-coordination geometry and is bonded to two heterocyclic N atoms, and an N atom and an O atom from Gly in a equatorial plane. The heterocyclic ligands behave as N,N′ bidentate ligands, and Gly ligand behaves as a N,O bidentate ligand. All of the complexes are positively charged, and neutralized by the free Cl^- anion located nearby. The positively charged complexes may have an advantage to interact with the negatively charged phosphate groups of DNA molecule. The typical coordination bond distances and angles are summarized in Table 2.

DNA Binding and Cleavage Studies The relative fluorescence intensity of EB was reduced by addition of the complexes into the EB-DNA solution. The extent of the fluorescence reduction of EB reflects the extent of binding of the complexes to DNA mainly by intercalation.[28,29] The binding property of the complexes to DNA is reflected by the slope of the quenching plot (Fig. 4). The extent of the binding of the complex **2** is predominant within three complexes. The values of the apparent binding constant (K_{app})[30,31] were deduced from the slope of the quenching plot according to the equation $K_{app,complex}[\text{Complex}]=K_{app,EB}[\text{EB}]$, where $K_{app,EB}$ is the apparent binding constant of EB assumed $10^7\,\text{M}^{-1}$ and [Complex] is the concentration of the complex at 50% quenching. $K_{app,complex}$ values were calculated as $2.2(1)\times10^5\,\text{M}^{-1}$, $2.7(2)\times10^5\,\text{M}^{-1}$ and $1.8(1)\times10^5\,\text{M}^{-1}$ for **1**, **2** and **3**, respectively. These results indicate that K_{app} value of **2** is larger than **1** and **3**, although K_{app} values of **1**, **2** and **3** are remarkably small as compared with that of EB. The DNA binding property can be reflected as the relative order: $[\text{Pd(Gly)(phen)}]^+\text{Cl}^-\cdot4\text{H}_2\text{O}$ (**2**)>$[\text{Pd(Gly)bpy)}]^+\text{Cl}^-\cdot4\text{H}_2\text{O}$ (**1**)>$\{[\text{Pd(Gly)(bpa)}]^+\text{Cl}^-\}_2\cdot6\text{H}_2\text{O}$ (**3**). These observations

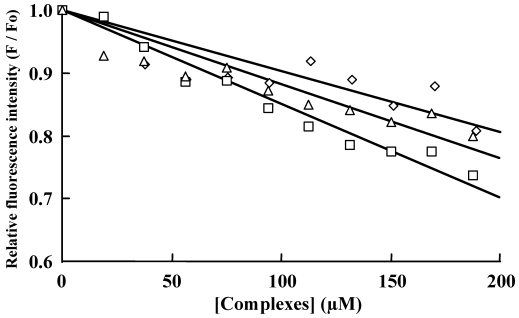

Fig. 4. Relative Fluorescence Intensity of the CT DNA-Bound Ethidium Bromide (9.00 μM) at Different Complex Concentrations in 10 mM Tris–HCl Buffer (pH7.4) Containing 50 mM NaCl at 25 °C on Addition of the Complexes: Complex **1** (△), Complex **2** (□), Complex **3** (◇)

The concentration of CT DNA was 93.2 μM. The excitation and emission wavelengths of EthBr were 545 nm and 600 nm respectively. F_0 and F represent the fluorescence intensity at 600 nm in the absence and presence of the complexes, respectively.

suggest that the three complexes compete with the intercalative EB binding to DNA in a different degree. Especially, **2** has a strong DNA binding ability as compared with the others.

The absorption spectra of the complexes in the presence of CT DNA are shown in Figs. 5a, b and c. Apparently large hypochromic effect of **2** was observed (Fig. 5b). On the other hand, the hypochromic effect of **1** (Fig. 5a) and **3** (Fig. 5c) was small and resemble each other.

Mital and Srivastava[32] studied the interaction of the ternary Pt(II) complex with phen and glycine, $[Pt(Gly)(phen)]^+$ with CT DNA using fluorescence method in the similar experimental conditions within this study, and suggested that the complex intercalates into CT DNA at low concentrations of the metal complex to nucleotide concentration, with external binding at higher complex concentrations after initial intercalation. The other several Pt(II) complexes with phen have been known to bind to DNA as intercalators.[33] The existence of the π–π interaction between phen planes in the crystal packing of **2** (Fig. 2b) suggests the formation of the intercalative binding. Further, in crystal structures of all complexes, the Cl^- anion is not coordinated to $[Pd(Gly)(X)]^+$. Therefore, positively charged complexes can easily interact with the negatively charged phosphate groups on DNA molecule.

Circular dichroism spectra shown in Fig. 6 were obtained using similar conditions as fluorescence and absorption measurements. The CD spectrum of CT DNA consists of a positive band at 275 nm a negative band at 245 nm, characteristic of DNA in right handed B form.[34] When **2** is incubated with CT DNA at $R=3$ which is enough to produce the absorption change (Fig. 5b), the CD spectrum of DNA undergoes the small red shift in the positive band at 275 nm and the reduction in the negative band at 245 nm. This spectral change is similar to that observed for DNA binding study[35] of Pt(II) complex of phen, $[Pt(phen)(en)]Cl_2$ (where en is ethylenediamine) at $R=1.1$ in the similar conditions with this study, in which the Pt(II) complex with phen is considered as the most efficient intercalator. The CD change also resembles that observed for DNA binding of Ni(II) complex of phen, [Ni(phen)(edda)] (where edda is *N*,*N*′-ethylenediaminediacetic acid)[36] at $R=1$, and that for the binding of altromycin B.[37] These compounds have been also considered as intercalators. The intercalation of the above compounds may be favored when the double helix adopts the A-conformation as reflected by the reduction at 245 nm.[37] On the other hand, complexes **1** and **3** did not show little changes of CD bands.

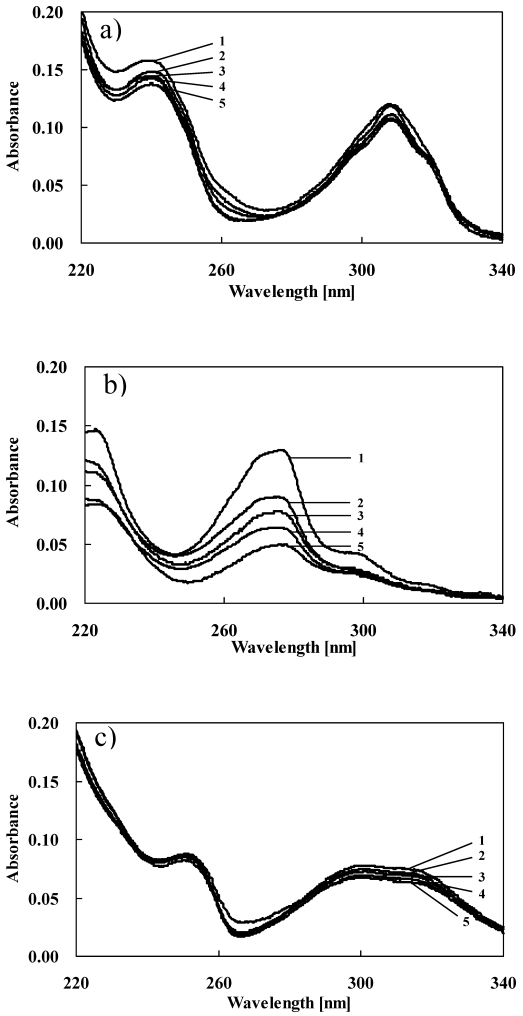

Fig. 5. Absorption Spectra of the Complexes (10 μM) in 10 mM Tris–HCl pH 7.4 and 50 mM NaCl, in the Absence and the Presence of Increasing Amounts of CT DNA at the Various Molar Ratio of DNA to the Complex (R=[DNA]/[Complex]) of: 1: 0, 2: 2, 3: 5, 4: 10 ; 5: 15

(a) Complex **1**, (b) complex **2**, (c) complex **3**.

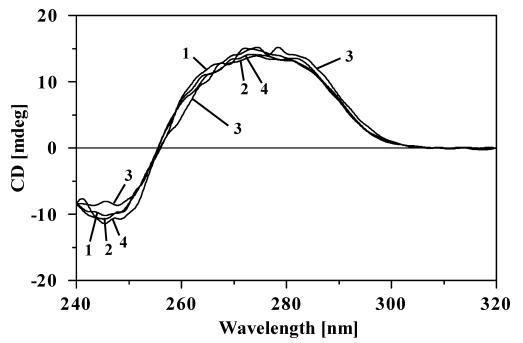

Fig. 6. Circular Dichroism Spectra of CT DNA on Its Interaction with the Complexes in 10 mM Tris–HCl pH 7.4 and 50 mM NaCl

The concentrations of CT DNA and the complexes are 150 μM and 50 μM, respectively (R=3). 1, CT DNA; 2, complex **1**; 3, complex **2**; 4, complex **3**.

The results of fluorescence, UV, CD and structural studies suggest that the complexes **1**, **2** and **3** bind to DNA, and, es-

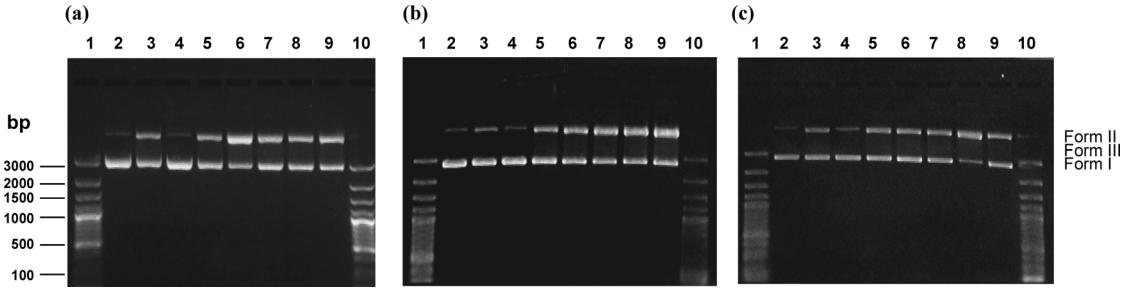

Fig. 7. Agarose Gel Electrophoresis of Cleavage of Plasmid pBR322 DNA (1 μg/40 μl) by the Palladium(II) Complexes in the Presence of H_2O_2 and Ascorbic Acid (H_2A) at 25 °C for 1 h, (a) Complex **1**, (b) Complex **2**, (c) Complex **3**

Lane: (1) and (10) marker; (2) DNA alone; (3) DNA+H_2O_2+H_2A; (4) DNA+complex (45 μM); (5) DNA+H_2O_2+H_2A+complex (15 μM); (6) 30 μM; (7) 45 μM; (8) 60 μM; (9) 75 μM. H_2O_2 and H_2A concentration is 525 μM.

pecially, **2** binds to DNA fundamentally by the intercalative binding mode. While the complexes **1** and **3** may bind to the groove of DNA. More precise DNA-binding modes of each complex will be proved by further studies.

The DNA cleavage ability of the complexes has also been investigated by gel electrophoresis using SC DNA. The electrophoretic migration patterns for the cleavage of SC DNA are usually characterized by three forms (Form I, II, III).[28,29,33,38] The fastest migration of the electrophoretic pattern is called Form I, which reflects super coiled DNA. A slower migration pattern is Form II, which reflects nicked circular DNA. Form III reflects linear open circular DNA, which migrates between Form I and Form II. Figure 7 shows the electrophoretic migration patterns of SC DNA in the presence and absence of the complexes, H_2O_2 and ascorbic acid. A little production of Form II was observed in the presence of H_2O_2 and ascorbic acid without complexes (lane 3). Control experiments using complex alone did not produce Form II even at a high concentration of 45 μM (lane 4). On the other hand, the apparent increase of Form II was observed by increasing concentrations of **2** in the presence of H_2O_2 and ascorbic acid (Fig. 7b, lanes 5—9). In the case of the complexes **1** and **3** (Figs. 7a and c, lanes 5—9), the conversion of Form I to Form II was also observed like **2**, but the concentration dependence of the migration pattern of **2** was clearer as compared with **1** and **3**. These electrophoretic results suggest that all of the complexes enhance the oxidative cleavage of SC DNA in the presence of H_2O_2 and ascorbic acid, although a little cleavage occures even in the presence of H_2O_2 and ascorbic acid without the complexes. Up to the present, the antibiotic activity of Pd(II) complexes with heterocyclic ligands has been reported *in vivo* and explained by the intercalation and/or groove binding models,[15,32,33,37,39] although the precise mechanism is not yet clear. Recently, the cleavage of Form I to Form II of the pUC19 plasmid DNA by the intercalative Pd(II) complex, $[Pd_2(\mu\text{-bzta})_4]\cdot 1.5DMSO$ (where bzta=benzothiazole-2-thiolate)[12] has been reported *in vitro*. Although the intercalative and/or groove binding of the Pd(II) complexes to DNA followed by the topological change of DNA may be an essential reason for the antibiotic activity of the complexes *in vivo*, the oxidative cleavage of SC DNA enhanced by the Pd(II) complexes in the presence H_2O_2 and ascorbic acid may be also worthy for considering the mechanisms of antibiotic activity of the Pd(II) complexes. More precise mechanistic aspects for the antibiotic activity of the Pd(II) complexes should be explored in further physicochemical studies.

Conclusion

The coordination modes of three ternary Pd(II) complexes with the different ligand atoms, N,O bidentate glycine ligand, and N,N′ bidentate heterocyclic ligand have been structurally characterized. The interaction between Pd(II) atom and ligand atoms are discussed including the packing effects.

DNA binding and cleavage ability of the complexes was also studied. Each of the complexes showed binding propensity to CT DNA, and enhanced cleavage activity for SC DNA in the presence of H_2O_2 and ascorbic acid. Complex **2**, $Pd(Gly)(phen)]^+Cl^-\cdot 4H_2O$ showed most effective DNA binding as compared with the complex **1** $[Pd(Gly)(bpy)]^+Cl^-\cdot 4H_2O$, and **3** $\{[Pd(Gly)(bpa)]^+Cl^-\}_2\cdot 6H_2O$. The physicochemical properties of the three ternary Pd(II) complexes clarified in this study are useful for further investigation of the biochemical behavior of this kind of Pd(II) complex.

Supplementary Material Crystallographic data for the structural analysis has been deposited with the Cambridge Crystallographic Data Centre, CCDC No. 639517 for $[Pd(Gly)(bpy)]^+Cl^-\cdot 4H_2O$ (1), CCDC639518 for $Pd(Gly)(phen)]^+Cl^-\cdot 4H_2O$, and CCDC 639519 for $\{[Pd(Gly)(bpa)]^+Cl^-\}_2\cdot 6H_2O$, respectively. Copies of this information may be obtained free of charge from The Director, CCDC, 12 Union Road, Cambridge, CB21EZ, U.K. (fax: +44–1223–336033; e-mail: deposit@ccdc.cam.ac.uk or www: http://www.ccdc.cam.ac.uk).

Acknowledgement We thanks Dr. M. Odoko of Kinki University for technical assistance.

References and Notes

1) Rosenberg B., Camp L. V., Trosko J. E., Mansour V. H., *Nature* (London), **222**, 385—386 (1969).
2) Wong E., Giandomenico C. M., *Chem. Rev.*, **99**, 2451—2466 (1999).
3) Abu-Surrah A. S., Al-Allaf T. A. K., Klinga M., Ahlgren M., *Polyhedron*, **22**, 1529—1534 (2003).
4) Tu C., Wu X., Liu Q., Wang X., Xu Q., Guo Z., *Inorg. Chim. Acta*, **357**, 95—102 (2004).
5) Anayive P. R., Vieites M., Gambino D., Piro O. E., Castellano E. E., Zani C. L., Souza-Fagundes E. M., Teixeira L. R., Batista A. A., Beraldo H., *J. Inorg. Biochem.*, **99**, 698—706 (2005).
6) Wang Y., Okabe N., *Chem. Pharm. Bull.*, **53**, 366—373 (2005).
7) Wang Y., Okabe N., *Chem. Pharm. Bull.*, **53**, 1291—1295 (2005).
8) Wang Y., Mizubayashi Y., Odoko M., Okabe N., *Acta Crystallogr.*, **C61**, m67—m70 (2005).
9) Muranishi Y., Okabe N., *Acta Crystallogr.*, **C60**, m47—m50 (2004).
10) Okabe N., Hagihara K., Odoko M., Muranishi Y., *Acta Crystallogr.*, **C60**, m150—m152 (2004).
11) Wang Y., Okabe N., Odoko M., *Chem. Pharm. Bull.*, **53**, 1291—1295 (2005).
12) Gao E.-J., Wang K.-H., Gu X.-F., Yu Y., Sun Y.-G., Zhang W.-Z., Yin H.-X., Wu Q., Zhu M.-C., Yan X.-M., *J. Inorg. Biochem.*, **101**, 1404—

1409 (2007).
13) Rebolledo A. P., Vieites M., Gambino D., Piro O. E., Castellano E. E., Zani C. L., Souza-Fagundes E. M., Teixeira L. R., Batista A. A., Beraldo H., *J. Inorg. Biochem.*, **99**, 698—706 (2005).
14) Mansuri-Torshizi H., Ghadimy S., Akbarzadeh N., *Chem. Pharm. Bull.*, **49**, 1517—1520 (2001).
15) Paul A. K., Mansuri-Torshizi H., Srivastava T. S., Chavan S. J., Chitnis M. P., *J. Inorg. Biochem.*, **50**, 9—20 (1993).
16) Mital R., Srivastava T. S., Parekh H. K., Chitnis M. P., *J. Inorg. Biochem.*, **41**, 93—103 (1991).
17) Puthraya K. H., Srivastava T. S., Amonkar A. J., Adwankar M. K., Chitnis M. P., *J. Inorg. Biochem.*, **25**, 207—215 (1985).
18) Shehata M., *Transition Met. Chem.*, **26**, 198—204 (2001).
19) Yodoshi M., Odoko M., Okabe N., *Chem. Pharm. Bull.*, **55**, 853—860 (2007).
20) Altomare A., Burla M., Camalli M., Cascarano G., Giacovazzo C., Guagliardi A., Moliterni A., Polidori G., Spagna R., *J. Appl. Crystallogr.*, **32**, 115—119 (1999).
21) Crystal Structure Analysis Package, Rigaku and Rigaku/MSC. 9009 New Trails Dr. The Woodlands TX 77381 U.S.A. (2000—2004).
22) Sheldrick G. M., SHELXL97. University of Göttingen, Germany (1997).
23) Le Pecq J. B., Paoletti C., *J. Mol. Biol.*, **27**, 87—106 (1967).
24) Waring M. J., *J. Mol. Biol.*, **13**, 269—282 (1965).
25) Mahadevan S., Palaniandavar M., *Inorg. Chem.*, **37**, 3927—3934 (1998).
26) Thomas A. M., Naik A. D., Nethaji M., Chakravarty A. R., *Inorg. Chim. Acta*, **357**, 2315—2323 (2004).
27) Reichman M. E., Rice S. A., Thomas C. A., Doty P., *J. Am. Chem. Soc.*, **76**, 3047—3053 (1954).
28) Baguley B. C., Bret M. L., *Biochemistry*, **23**, 937—943 (1984).
29) Lakowicz J. R., Weber G., *Biochemistry*, **12**, 4161—4170 (1973).
30) Dhar S., Nethaji M., Chakravarty A. R., *Dalton Trans.*, **2004**, 4180—4184 (2004).
31) Lee M., Rhodes A. L., Wyatt M. D., Forrow S., Hartley J. A., *Biochemistry*, **32**, 4237—4245 (1993).
32) Mital R., Srivastava T. S., *J. Inorg. Biochem.*, **40**, 111—120 (1990).
33) Howe-Grant M., Lippard S. J., *Biochemistry*, **18**, 5762—5769 (1979).
34) Selvakumar B., Rajendiran V., Maheswari P. U., Stoeckli-Evans H., Palaniandavar M., *J. Inorg. Biochem.*, **100**, 316—330 (2006).
35) Brodie C. R., Collins J. G., Aldrich-Wright J. R., *Dalton Trans.*, **2004**, 1145—1152 (2004).
36) Ng C. H., Kong K. C., Von S. T., Balraj P., Jensen P., Thirthagiri E., Hamada H., Chikira M., *Dalton Trans.*, **2008**, 447—454 (2008).
37) Nikolis N., Methenitis C., Pneumatikakis G., *J. Inorg. Biochem.*, **95**, 177—193 (2003).
38) Li H., Le X.-Y., Pang D.-W., Deng H., Xu Z.-H., Lin Z.-H., *J. Inorg. Biochem.*, **99**, 2240—2247 (2005).
39) Cusumano M., Giannetto A., *J. Inorg. Biochem.*, **65**, 137—144 (1997).